ASM Sci. J.Special Issue 2018(1) AiMS2018, 75-85

Structural and Optical Properties of Heat Treated Zn_2SiO_4 Composite Prepared by Impregnation of ZnO on SiO_2 Amorphous Nanoparticles

E. A. G. Engku Ali[1,2,3*], K. A. Matori[3], E. Saion[4], S. H. A. Aziz[4], M. H. M. Zaid[4] and I. M. Alibe[4]

[1]*School of Fundamental Science, Universiti Malaysia Terengganu, 21030 Kuala Nerus, Terengganu, Malaysia.*

[2]*Advanced Nano Materials (ANoMa) Research Group, Universiti Malaysia Terengganu, 21030 Kuala Nerus, Terengganu, Malaysia.*

[3]*Materials Synthesis and Characterization Laboratory, Institute of Advanced Technology, Universiti Putra Malaysia, 43400 UPM Serdang, Selangor*

[4]*Department of Physics, Faculty of Science, Universiti Putra Malaysia, 43400 UPM Serdang, Selangor, Malaysia.*

In this study, Zn_2SiO_4 composite-based ceramic was synthesised using amorphous SiO_2 nanoparticles as a silicon source. Different ratios of Zn:Si were prepared by mixing amorphous SiO_2 nanoparticles with aqueous zinc nitrate. Amorphous SiO_2 nanoparticles were encapsulated by the zinc source in aqueous solution, dried, and subjected to heat treatment. The heat treatment underwent by the amorphous SiO_2 nanoparticles, with zinc source mixture, showed the changing of phases, morphology, and size with increased temperature. ZnO phase appeared at the beginning of heat treatment and Zn_2SiO_4 phase started to emerge at 800°C onwards, as shown by XRD patterns. The average crystallite size increases from 37 nm at 600 °C to 68 nm at 1000 °C. The spherical morphology was observed at 600 and 700 °C, but at temperatures higher than 800 °C, the dumbbell or necking-like structures formed. Optical band gap analysis of Zn_2SiO_4 composite was determined to be within the range of 3.12 ± 0.04 to 3.17 ± 0.04 eV. The photoluminescence of treated samples showed emission peaks at 411 and 455 nm wavelengths from ZnOs blue band and at 528 nm wavelength from Zn_2SiO_4′s green band. The diffusion of zinc ions into Zn_2SiO_4 composite with high surface area will favour the diffusion at a much lower temperature compared to a conventional solid state method.

Keywords: Zinc silicate, oxide materials, photoluminescence, amorphous silica, nanoparticles

I. INTRODUCTION

In recent years, interest on the synthesis and analysis of Zn_2SiO_4 composite has grown due to its potential in display devices, detector systems, such as X-ray screens and scintillators, and for luminous paint, or coating. Previous studies have focused on improving synthetic methods, and using low cost, less hazardous precursor ma-

*Corresponding author:engku_ghapur@umt.edu.my

terials. Traditionally, Zn_2SiO_4 is prepared using a solid state reaction method by applying heat treatment to a mixture of zinc oxide (ZnO) and silica (SiO_2) as the precursors [1]. The physical, chemical, and optical properties of the resulting Zn_2SiO_4 depend on the preparation method and starting materials. As for silicate-based phosphor, the selection of silica precursors can certainly influence the final properties of the targeted materials.

Other from the laboratory grade SiO_2, soda lime silica produced from waste materials [2]-[3], silicon alkoxide, or tetraethyl orthosilicate (TEOS) [4], and commercialized mesoporous SiO_2 are among common SiO_2 sources [5]. The conventional melt quenching of soda lime silica, mixed with ZnO, produces a glass precursor, which is then subjected to heat treatment to form Zn_2SiO_4-based glass-ceramic.

The drawback of using soda lime silica is the presence of other elements in the glass, which can affect the properties of the final materials [6]. Sol gel, hydrothermal and vapour method require a specific materials or equipment in order to prepare the samples. Requirements such as soluble precursors for gel-like system [7], a Teflon-lined autoclave to heat the mixtures for hydrothermal method and a chamber or container for vapour method is needed for produce the materials [8]-[9].

The use of silica, whether solid or porous particles as a precursor, has the possibility of adopting other methods that favour simple process routes and lower cost. This technique provided a simple preparation route that did not require special equipment during synthesis [10]. The use of solid silica mixed with a source of zinc ions in an aqueous state can influence some of the properties and changes in the phase formation temperature. Porous or mesoporous materials have been used to synthesise materials or compounds that can form new functional phases that will improve the properties of the initial source material. In this study, the wet chemical impregnation method, combined with sintering, was used to synthesise Zn_2SiO_4 composite. Solid SiO_2 nanoparticles were used as a template and mixed with a solvent containing dissolved zinc ions from zinc nitrate hexahydrate.

II. MATERIALS AND METHODS

The synthesis of SiO_2 nanoparticles powder are prepared according to the procedure presented in earlier report [11]. Zn_2SiO_4 composite powders were produced by mixing amorphous silica nanoparticles that were produced previously with zinc nitrate hexahydrate. First, 1.20 g of amorphous silica nanoparticles was dispersed in 200 mL of deionized (D.I.) water using an ultrasonic agitator for 30 minutes. Next, the amorphous silica nanoparticle dispersion was mixed with a solution of 11.89 g of zinc nitrate hexahydrate (Sigma Aldrich), which was already dissolved in 200 mL of deionized water. This mixture was stirred for 2 hours using a magnetic

stirrer. The ratio of the precursor concentration of Zn:Si are 2:1, 1.75:1, 1.5:1 and 1.25:1. Then, the mixed solution was poured into a petri dish and dried in an oven for 24 hours at 120 °C. The dried powder was ground using a mortar grinder and finally, heat treated at 600, 700, 800, 900, and 1000 °C at 10 °C /min heating rate for 3 hours.

To study the structural characteristic of synthesised Zn_2SiO_4 composite, the sample powder was characterized by X-ray diffraction (XRD) (PANalytical X′pert PRO PW 3040 MPD), field emission scanning electron microscopy (FESEM) (FEI NOVA NanoSEM 230) and Fourier Transform Infrared reflection (FTIR) spectrometer (Perkin Elmer Spectrum 100) with universal attenuated total reflectance (ATR) between the wavenumber of 400 to 4000 cm^{-1}. In addition, the optical property was characterized using UV-Visible (Shimadzu UV-3600) spectrometer with absorption signal was measured between 200 to 800 nm wavelengths for optical absorption and band gap determination. The diffuse reflectance measurements give the reflectance values of the sample. To further analyse the optical properties of the sample, the Kubelka-Munk model was used to determine the absorption coefficient using the specific software that came with the UV-Vis equipment. Perkin Elmer LS 55 Fluorescence Spectrometer was used in the photoluminescence characterization analysis and the wavelength of 350 nm was chosen to excite the material.

III. RESULTS AND DISCUSSIONS

A. XRD analysis

Figures 1 shows the XRD spectra of heat treated Zn_2SiO_4 composite were recorded in the range $2\Theta = 10°$ to 80° form 600 to 1000 °C. The wurtzite structure of the ZnO nanocrystals was observed at 600 °C. Nine major diffraction peaks were positioned at 2Θ values that corresponded to the X-ray diffraction planes of ZnO wurtzite crystal structure (JCPDS No. 89-0510). The lattice constant calculated from the XRD spectrum gave the value of a = 3.249 Å and c = 5.206 Å, which were similar to ZnO hexagonal wurtzite structure [12].

Diffraction peaks had broadened and shifted towards the higher angle side with increased of sintering temperature. When the size of ZnO nanocrystals had increased, its growth might has been interrupted by the surrounding SiO_2 matrix and porous nature of the SiO_2 nanopowder. As a result, the diffraction peaks of ZnO were shifted towards the higher angle side, with increases in temperature that related to the strain induced in the ZnO nanocrystals by the surrounding silica network [13].

At 700 °C, the small peaks of Zn_2SiO_4 phase started to form and became obvious at 800 °C that corresponded to α-Zn_2SiO_4 crystal phase (JCPDF No. 37-1485). The formation of Zn_2SiO_4 crystal phase at 700 °C was influenced by the ZnO, which became the dominant dif-

fusion species during thermal annealing due to its lower activation energy of surface diffusion [14]. The activation energy was gained rapidly with the increase in temperature. The zinc ions on the surface of the SiO_2 nanoparticles had diffused and formed Zn_2SiO_4 at lower temperatures. Furthermore, using SiO_2 nanoparticles, which contained silanols, amorphous in structure and large surface area has led to the lowering of the formation temperature [5]

Additionally, the impregnated ZnO on the surface of silica nanoparticles has low surface diffusion activation energy. The lower activation energy (158 kJ/mol) of the ZnO surface diffusion compared to the bulk diffusion (347-405 kJ/mol) will primarily diffuse the ZnO atoms at the surface towards the silica matrix and promote the formation of Zn_2SiO_4 crystal phase [15]. During this time, the splitting of zinc oxide peak at 31.79° and 34.44°, which shifted to lower 2Θ was also observed. The rise in temperature had immediately increased the diffusion. Hence, Zn_2SiO_4 crystal phase formation had proceeded with the increase in sintering temperature and at 1000 °C, Zn_2SiO_4 became the main crystal phase and the intensity of ZnO peak had decreased. The single phase of Zn_2SiO_4 was likely to have been formed with a small amount of ZnO trace was still available at 1000 °C.

The full width at half maximum (FWHM) values were used to calculate the average crystallite size using the Scherrer′s equation [16]

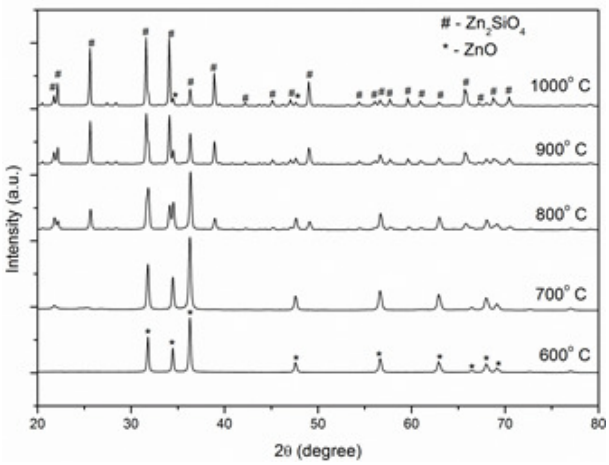

Figure 1. XRD pattern of Zn_2SiO_4 composite, heat treated between 600 to 1000 °C.

$$D = \frac{k\lambda}{\beta cos\Theta} \text{.....(1)}$$

where k = Scherrer constant depends on the how the width is determined, the shape of the crystal and the size distribution, λ is the X-ray wavelength (1.5418 Å), β is full width at half maximum in radians (FWHM) and Θ is Bragg angle in degree. As the heat treatment temperature had increased, the average calculated crystallite size of ZnO, has also increased (Table 1). At 600 °C, the average crystallie size was approximately 37 nm, and increased between the ranges of 68 nm at 1000 °C of heat treatment. The average crystallite size of Zn_2SiO_4 crystal phase of the same samples had similar increments of crystallite size values with increasing temperature.

The lattice constant of Zn_2SiO_4 phase calculated from the sintered sample was about a $\sim$ 13.932 Å and c $\sim$ 9.257 Å, which was close to the values obtained by Ghoul and Mir (2015), who used sol-gel technique with TEOS as a sil-

ica precursor [16]. The increasing temperature has made the Zn and Si ions to become moveable at the contact surface due to the increased energy. These ions tend to diffuse and move into the SiO_2 nanoparticles, thus forming Zn_2SiO_4 phase.

Table 1. The average crystallite size of ZnO and Zn_2SiO_4 at various sintering temperatures.

Temperature (°C)	Average crystallite size (nm)	
	ZnO	Zn_2SiO_4
600	37.30	-
700	40.30	-
800	42.12	43.51
900	54.29	45.40
1000	66.05	52.09

B. FTIR analysis

Figure 2 shows the FTIR spectra of Zn_2SiO_4 composites sintered at various temperatures. The sample that was dried at 120 °C showed IR bands at 3600 cm^{-1} and 1600 cm^{-1}, which can be attributed to the O-H stretching vibrations and bending modes of adsorbed water. The presence of organic molecules were represented by the IR bands at 1300 cm^{-1} for C-H bond and 1320 cm^{-1} (weak shoulder peak) for NO_3^- bond. This bond can be referred to nitrate ions in nitrate and some organic contaminants that were in the precursors and de-ionized water. The mixture of Zn and Si ions was added with hydrolysed zinc nitrate and SiO_2 nanoparticle powder in deionized water from the previous preparation step. Yang *et al.* (2008) reported that the electrostatic force could influence $Zn(OH)SiO_2$ colloidal particles to be absorbed onto SiO_2 nanoparticles [17].

At 600 °C, the entire organic and hydroxyl bonds have disappeared. Meanwhile, the IR bands that existed for all heat treated samples were observed at 1050 to 1100 cm^{-1}, 790 to 880 cm^{-1}, and 410 to 360 cm^{-1} assigned to the asymmetric stretching modes of Si-O-Si vibrations, symmetric stretching of ZnO_4, and ZnO stretching band. The amorphous nature of silica dried at elevated temperatures prompted the availability of silanol or hydroxyl groups. These water-related molecules were present at the surface, as well as within the pores inside the particle structure [18]. When the hydroxyl groups at the surface of the silica particles became condensed, the dangling bonds on the silica surface would attach to the zinc phase in ZnO. This would allow the consolidation and diffusion to occur between SiO_2 and ZnO atoms. With progressive sintering temperature, the intensity of the 1056 cm^{-1} peak had gradually decreased and shifted to 1110 cm^{-1}. This result suggested that Si atoms were replaced by Zn ions to form Si-O-Zn bonds [19].

New vibrational bands were observed at 570 to 600 cm^{-1}, linked to the symmetrical vibrations of the ZnO_4 group [20]. The group of vibrational bands observed between 790 and 880 cm^{-1} had also increased with increasing temper-

ature, which can be attributed to SiO_4 tetrahedron vibration. The presence of vibrational bands of SiO_4 and ZnO_4 groups suggests the formation of the Zn_2SiO_4 phase [21]. The bands for asymmetrical stretching of Si-O-Si and ZnO had decreased, which indicated that the Si-O-Si and ZnO bonds were broken during the conversion to Zn_2SiO_4.

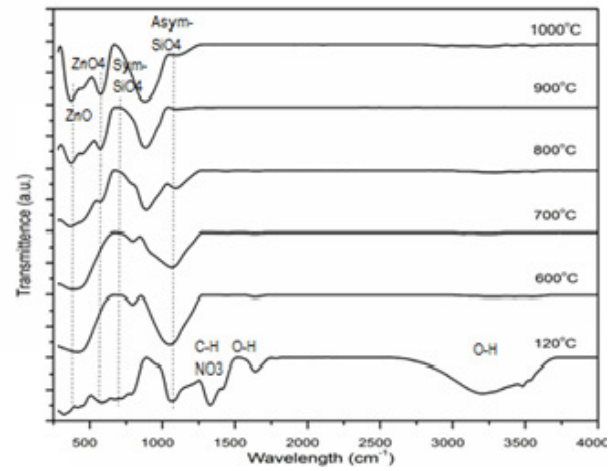

Figure 2. FTIR spectral pattern of heat treated Zn_2SiO_4 composite at a temperature ranging from 600 to 1000 °C.

C. FESEM analysis

Figure 3 shows FESEM images of samples exhibited spherical morphology at 600 and 700 °C, but at temperatures of higher than 800 °C, the dumbbell or necking-like structures were formed. The overall morphology of Zn_2SiO_4 composite, upon annealing at 600 °C, showed the spherical form with an average diameter of 69.68 ± 3.20 nm. Some parts of the composite displayed individual particles, while other parts showed agglomeration. Burned off residual organic groups, such as nitrates, could lead to the encapsulation of ZnO on the surface of SiO_2 nanoparticles and the particle size cannot be precisely estimated from annealing at 700 °C [14]. For the sample that was heat treated at 800 °C and higher, the particles appeared to be diffusing into one another. At 1000 °C, the melting-like morphology was observed [22]. The formation of bulky structures at this temperature could possibly be due to the tendency of the spherical particles to minimize their surface energy by diffusing with one another at elevated temperatures.

D. UV-Vis spectroscopy analysis

Figures 4 shows the absorption spectra of the UV-Visible for heat treated Zn_2SiO_4 composite recorded in the spectral region of 200 to 800 nm. The maximum absorption edge of the heat treated samples was at approximately 380 nm. This sharp absorption edge correlate to the characteristics of the crystalline phase of ZnO. For sample heat treated at 600 °C, when the ratio of zinc was decreased, the absorption intensity became lower. Gun′Ko *et al.* (2013) suggested that the intensity of the band was highly depended on the content of zinc oxide [23].

E. Optical band gap analysis

The electronic transitions of crystalline or non-crystalline materials can be studied by

analysing the resulting optical absorption coefficient (α) near the absorption edge. The experimental optical band gap can be obtained by using equation $(\alpha h\nu)^{1/n} = A(h\nu - E_g)$, where A is a constant, the photon energy is denoted by $h\nu$, and E_g is the optical energy band [3],[24]. The determination of optical band gap value from the best linear fit by extrapolating the linear parts of $((\alpha h\nu)^{1/n}$ vs. $h\nu$ curves is done by using n = 1/2 which is value for direct allowed transition. The x-axis interception from extrapolation of linear region of individual plot lines gave optical band gap value as shows in Figure 5. The band gap for ZnO of heat treated sample in the range of 3.12±0.04 to 3.17±0.04 eV, compared to the bulk band gap which is 3.37 eV. Sidek *et al.* (2009) emphasised that optical band gap decreased with the additional of non-bridging oxygen (NBO) in the TeO-ZnO system [25]. The symmetrical vibration of the ZnO_4 and SiO_4 group observed in FTIR spectra with increasing of temperature causes the increment of NBO. The shift in UV absorption band is noticeably from NBO that bound an excited electron lesser than bonding oxygen (BO). This factor contributes to the variation in optical band gap of the heat treated samples. The higher sintering temperature also had increased the particle size and became denser structure with less pores, due to diffusing of articles with one to another as shown in FESEM micrographs that could lead to higher absorbance of photons [26].

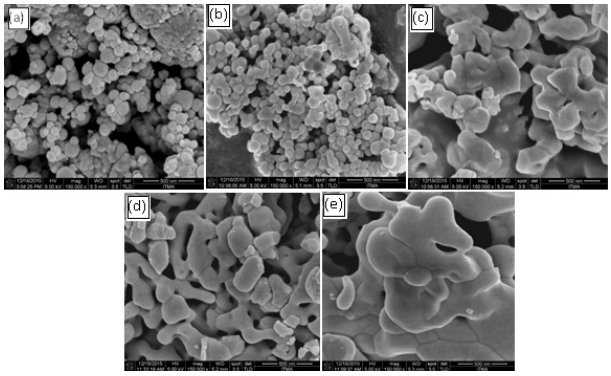

Figure 3. FESEM micrographs of Zn_2SiO_4 composite heat treated at: (a) 600°C; (b) 700 °C; (c) 800 °C; (d) 900 °C; and (e) 1000 °C.

F. Photoluminescence analysis

Figures 5 shows the emission spectra of Zn_2SiO_4 composites with the increase of heat treatment. Several peaks were observed at the particular wavelength, with differences in intensities. Based on the XRD spectra, the higher heat treatment temperature would increase the crystallinity of the ZnO and Zn_2SiO_4 phases. By applying the Gaussian fitting, four peaks can be resolved from the spectra, observed at 411, 455, 480, and 528 nm wavelengths. The near-violet emission at 411 nm of the ZnO-Zn_2SiO_4 composite was reported by Vaishnavi *et al.* (2008) suggested that the interface traps in the depletion region were due to the oxygen vacancies at the ZnO-SiO_2 interface formation in the [27]. The blue emission at 455 and 480 nm wavelengths attributed to oxygen vacancies inside ZnO crystallites and interstitial oxygen. The photoluminescence intensity was reduced when the samples were heat treated at higher than 700 °C,

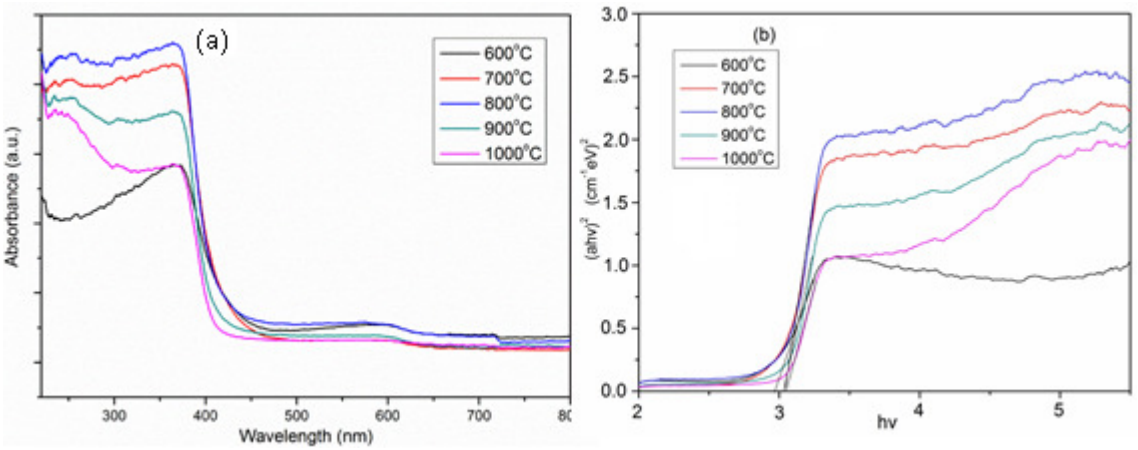

Figure 4. (a) UV-Vis absorption spectra for Zn_2SiO_4 composite, sintered from 600 to 1000 °C. (b) Tauc plot of $(\alpha h\nu)_2$ vs. energy for Zn_2SiO_4 composite, with Zn:Si ratio of 1.25:1, sintered at 600 to 1000 °C using SiO90m.

which was caused by the reduction in oxygen vacancies. At 1000 °C, the emission peak at 528 nm had increased for all treated samples. He *et al.* (2003) suggested that although the formation of Zn_2SiO_4 can be detected after undergoing high heat treatment temperature (higher than 900 °C), the Zn_2SiO_4 phase did not contribute to the emission of the green band [28]. The green band emission was indicated as the transition of the photoexcited electron from the conduction band edge to an oxygen vacancy in ZnO. In this study, it is apparent that no activator was used on the host material. The emission at 528 nm can be related to the changing of energy schematic of ZnO and the defects generated by the neighbouring crystal field of Zn_2SiO_4 during heat treatment.

IV. SUMMARY

In this study, Zn_2SiO_4 composites were successfully prepared by sintering the mixture of SiO_2 nanoparticles with aqueous zinc nitrate. The formation of Zn_2SiO_4 composite was observed when the temperature was increased to higher than 800 °C, which was lower than conventional solid state sintering temperature. The average crystallite size increases from 37 nm at 600 °C to 68 nm at 1000 °C. The impregnation of zinc ions with amorphous SiO_2 nanoparticles had significantly reduced the formation temperature of Zn_2SiO_4 phase. The Zn-O and Si-O-Zn vibration bands in the FTIR transmittance spectra shows the characteristics of Zn_2SiO_4 phase formation. Based on the morphological analyses from FESEM, as the temperature increases, the spherical particles exhibited interconnections between the particles. UV-Vis mea-

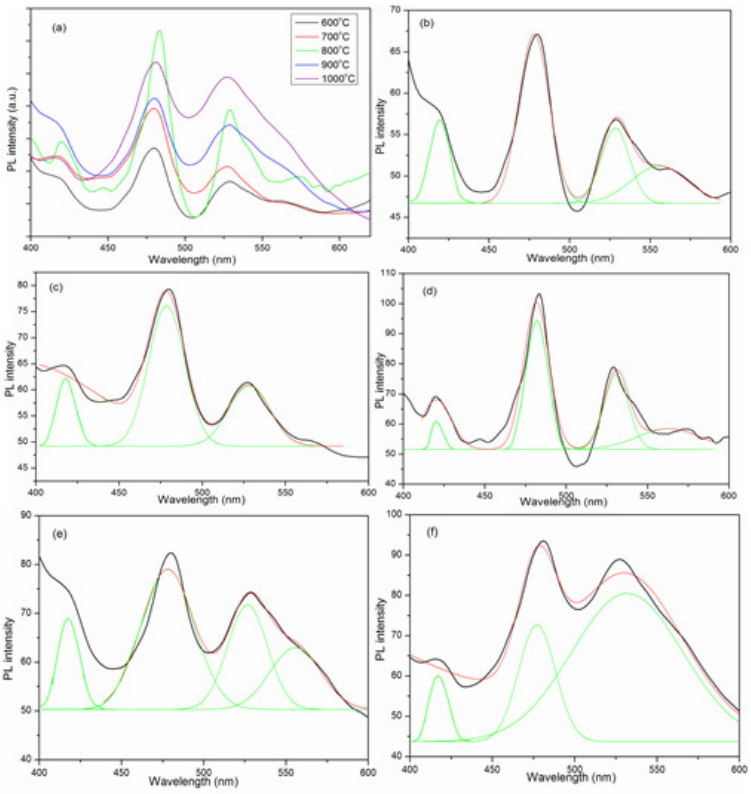

Figure 5. Photoluminescence spectra of: (a) Zn_2SiO_4 composite, sintered at various temperatures, and Gaussian fitting for samples sintered at: (b) 600 °C: (c) 700 °C: (d) 800 °C: (e) 900 °C; and (f) 1000 °C using SiO90m excited at 355 nm wavelength.

surements showed the values of the calculated optical band gap of ZnO to be in the range of 3.12±0.04 to 3.17±0.04 eV. The photoluminescence spectra showed the emission of near violet, blue, and green bands. The intensity of band emission was mostly influenced by the heat treatment temperature. The synthesised Zn_2SiO_4 composite had shown as a promising candidate for phosphor materials. Its optical properties appeared suitable to be further developed for applications in photonic and optoelectronic materials.

V. ACKNOWLEDGMENT

The authors gratefully acknowledged the financial support for this study from the Malaysian Ministry of Higher Education (MOHE), Universiti Malaysia Terengganu and Universiti Putra Malaysia.

[1] Takesue, M, Hayashi, H, Smith, RL, 2009, Thermal and chemical methods for producing zinc silicate (willemite): A review. *Progress in Crystal Growth and Characterization of Materials*,

vol. 55(3-4), pp. 98-124.

[2] Samsudin, NF, Matori, KA, Abdul Wahab, Z, Josephine, YCL, Fen, YW, Hj Ab Aziz, S, Zahid, MHM, 2016, Low cost phosphors: Structural and photoluminescence properties of $Mn2^{+}$-doped willemite glass-ceramics. *Optik - International Journal for Light and Electron Optics*, vol. 127(19), pp. 8076-8081.

[3] Zaid, MHM, Matori, KA, Aziz, SHA, Kamari, HMM, Wahab, ZA, Effendy, N, Alibe, IM, 2016, Comprehensive study on compositional dependence of optical band gap in zinc soda lime silica glass system for optoelectronic applications, *Journal of Non-Crystalline Solids*, vol. 449, pp. 107-112.

[4] Lu, Q, Wang, P, Li, J, 2011, Structure and luminescence properties of Mn-doped ZnO-SiO_2 prepared with extracted mesoporous silica, *Materials Research Bulletin*, vol. 46, pp. 791-795.

[5] Li, Z, Zhang, H, Fu, H, 2013, Facile synthesis and morphology control of ZnO-SiO_2:Mn nanophosphors using mesoporous silica nanoparticles as templates. *Journal of Luminescence*, vol. 135, pp. 79-83.

[6] Zaid, MHM, Matori, KA, Abdul Aziz, SH, Zakaria, A, Ghazali, MSM, 2010, Effect of ZnO on the physical properties and optical band gap of soda lime silicate glass. *International Journal of Molecular Sciences*, vol. 13, pp. 7550-7558.

[7] Petrovykh, KA, Rempel, AA, Kortov, VS, Buntov, EA, 2015, Sol-gel synthesis and photoluminescence of ZnO-SiO_2:Mn nanoparticles. *Inorganic Materials*, vol. 51(2), pp. 152-157.

[8] Yu, X, Wang, Y, 2009, Synthesis and VUV spectral properties of nanoscaled ZnO-SiO_4:$Mn2^{+}$ green phosphor. *Journal of Physics and Chemistry of Solids*, vol. 70(8), pp. 1146-1149.

[9] Wang, WC, Tian, YT, Li, K, Lu, EY, Gong, DS, Li, XJ, 2013, Capacitive humidity-sensing properties of ZnO-SiO_4 film grown on silicon nanoporous pillar array. *Applied Surface Science*, vol. 273, pp. 372376.

[10] Taghavinia, N, Lerondel, G, Makino, H, Yamamoto, A, Yao, T, Kawazoe, Y, Goto, T, 2001, Nanocrystalline ZnO-SiO_4:$Mn2^{+}$ grown in oxidized porous silicon, *Nanotechnology*, vol. 12, pp. 547-551.

[11] Engku Ali EAG, Matori KA, Saion E, Sidek HAA, Zaid MHM, Alibe IM, 2017, Effect of Reaction Time on Structural and Optical Properties of Porous SiO2 Nanoparticles, Digest. *Journal of Nanomaterials and Biostructures*, vol. 12, pp. 441-447.

[12] Omri, K, Ghoul, JE, Alyamani, A, Barthou, C, Mir, LE, 2013, Luminescence properties of green emission of SiO_2/ZnO-SiO_2:Mn nanocomposite prepared by sol-gel method, *Physica E: Low-Dimensional Systems and Nanostructures*, vol. 53, pp. 48-54.

[13] Raevskaya, AE, Panasiuk, YV, Stroyuk, OL, Kuchmiy, SY, Dzhagan, VM, Milekhin, AG, Yeryukov, NA, Sveshnikova, LA, Rodyakina, EE, Plyusnin, VF, Zahn, DRT, 2014, Spectral and luminescent properties of ZnO-SiO_2 core-shell nanoparticles with size-selected ZnO cores, *RSC Advances*, vol. 4(108), pp. 63393-63401.

[14] Babu, KS, Reddy, AR, Reddy, KV, 2014, Controlling the size and optical properties of ZnO nanoparticles by capping with SiO2, *Materials Research Bulletin*, vol. 49, pp. 537-543 .

[15] Tomlins, GW, Routbort, JL, Mason, TO, 1998, Oxygen diffusion in single-crystal zinc oxide, *Journal of the American Chemical Society*, vol. 81, pp. 869-876.

[16] Ghoul, JE, Mir, LE, 2015, Synthesis by sol-gel process, structural and luminescence of V and Mn doped α-Zn_2SiO_4, *Journal of Materials Science: Materials in Electronics*, vol. 26, pp. 3550-3557.

[17] Yang, H, Xiao, Y, Liu, K, Feng, Q, 2008, Chemical precipitation synthesis and optical properties of ZnO/SiO_2 nanocomposites, *Journal of the American Ceramic Society*, vol. 91(5), pp. 1591-1596.

[18] Mody, HM, Kannan, S, Bajaj, HC, Manu, V, Jasra, RV, 2008, A simple room temperature synthesis of MCM-41 with enhanced thermal and hydrothermal stability, *Journal of Porous Materials*, vol. 15(5), pp. 571-579.

[19] Grigorie, AC, Muntean, C, Vlase, T, Locovei, C, Stefanescu, M, 2016, ZnO-SiO_2 based nanocomposites prepared by a modified sol-gel method, *Materials Chemistry and Physics*, vol. 186, pp. 399-406

[20] Ramakrishna, PV, Murthy, DBRK, Sastry, DL, Samatha, K, 2014, Synthesis, structural and luminescence properties of Mn doped ZnO/Zn2SiO4 composite microphosphor, *Spectrochimica Acta Part A: Molecular and Biomolecular Spectroscopy*, vol. 129, pp. 274-279.

[21] Podbrscek, P, Drazic, G, Anzlovar, A, Orel, ZC, 2011, The preparation of zinc silicate/ZnO particles and their use as an efficient UV absorber, *Materials Research Bulletin*, vol. 46(11), pp. 2105-2111.

[22] Rasdi, NM, Fen, YE, Azis, RS, Omar, NAS, 2017, Photoluminescence studies of cobalt (II) doped zinc silicate nanophosphors prepared via sol-gel method, *Optik*, vol. 149, pp. 409-415.

[23] Gun′Ko, VM, Bogatyrov, VM, Oranska, OI, Borysenko, LI, Skubiszewska-Zieba, J, Ksiazek, A, Leboda, R, 2013, Structural features of ZnxOy/nanosilica composites, *Applied Surface Science*, vol. 276, pp. 802-809.

[24] Tan, GL, Lemon, MF, Jones, DJ, French, RH, 2005, Optical properties and London dispersion interaction of amorphous and crystalline SiO_2 determined by vacuum ultraviolet spectroscopy and spectroscopic ellipsometry, *Physical Review B - Condensed Matter and Materials Physics*, vol. 72, pp. 1-10.

[25] Sidek, HAA, Rosmawati, S, Talib, ZA, Halimah, MK, Daud, WM, 2009, Synthesis and optical properties of ZnO-TeO_2 glass system. *American Journal of Applied Sciences*, vol. 6(8), pp. 1489-1494.

[26] Kumar, S, Sahare, PD, 2012, Observation of band gap and surface defects of ZnO nanoparticles synthesized via hydrothermal route at different reaction temperature, *Optics Communications*, vol. 285, pp. 5210-5216.

[27] Vaishnavi, TS, Haridoss, P, Vijayan, C, 2008, Optical properties of zinc oxide nanocrystals embedded in mesoporous silica, *Materials Letters*, vol. 62, pp. 1649-1651

[28] He, H, Wang, Y, Zou, Y, 2003, Photoluminescence property of ZnO-SiO_2 composites synthesized by sol-gel method, *Journal of Physics D: Applied Physics*, vol. 36(23), pp. 2972-2975.